

# STAINLESS STEEL RF DRY LOAD WITH SUPPRESSING SURFACE ELECTRIC FIELD

A. Lounine, T. Higo<sup>1</sup> and N. Kudo, KEK, Tsukuba, Japan  
K. Watanabe, The Graduate University for Advanced Studies, Hayama, Japan

## Abstract

An X-band RF dry load made of magnetic stainless steel, SS430, was designed to work at a low surface electric field. The optimization process of the lossy section was performed using an S-matrix formalism and the maximum surface electric field is below 55MV/m at an input power of 100MW. A new elliptical polarizer was proposed making a smooth transition from the linearly polarized point at the input of the load to the circularly polarized point at the entrance to the lossy region. This design suppresses the local enhancement of the electromagnetic field, resulting in a very broad bandwidth of 1 GHz below -20dB.

Based on this design, a test load was fabricated. It was clarified that the surface resistance of the magnetic stainless steel SS430 was decreased by a factor of ~1.2 due to the high temperature brazing process. This load has been high-power tested at XTF of KEK at 50MW.

## 1 INTRODUCTION

RF dry loads are preferred because no worry about the water leakage into vacuum side. At the X-band high power use, many of the existing dry loads took smooth taper design. This case a finite length is needed for matching performance.

A stainless-steel high power X-band RF load was proposed at SLAC in 1995 [1] which utilized resonant mode in a self-matched lossy load cells. This design opened the potential to make loads compact. Many loads of this design have been in operation for months at SLAC at the linear collider test facility [2,3]. KEK imported some loads and also fabricated one. These loads were used in high power at up to several tens of MW and with a pulse width ranging from 100ns to 1.6 microsec. In this usage, we sometimes encountered breakdowns in the load [4]. The similar breakdown behaviour was observed at SLAC at the upstream part of the lossy region [5].

Since the electric field of the original SLAC design at the upstream is larger than those of downstream, we suspect that the high electric field there is the cause of the breakdowns. The edge of the groove is fairly sharp and this is also one of the causes. In the present paper, we improved the design by reducing the surface electric field not only the lossy material region stated above but also the transformer part upstream of the lossy region.

## 2 DESIGN

### 2.1 Schematic shape of the present load

A schematic shape of the present load is shown in Fig. 1. It is composed of the upstream mode converter followed by a series of lossy load cells. The mode converter changes firstly the TE<sub>11</sub> mode in the rectangular wave guide to the TE<sub>11</sub> mode in the circular wave guide. Then it converts the linearly polarized TE<sub>11</sub> mode to the circularly polarized TE<sub>11</sub> mode when passing through an elliptical cross section with the axis 45 degrees rotated with respect to the original linear polarization axis. The lossy section is made of magnetic stainless steel, SS430, which has a large surface resistance at 11.4GHz, 19 times higher than copper [6]. Each cells are self-matched block with a pair of chokes, in which RF loss is enhanced in a resonant-like excitation of TM-like mode.

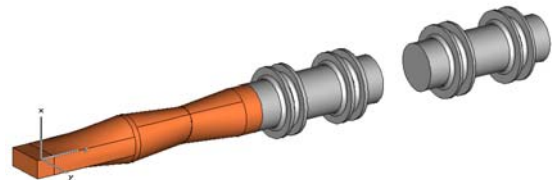


Fig. 1 Schematic of the load.

### 2.2 Lossy cell shape

The basic structure of each lossy load cell is shown in Fig. 2. The circular pipe diameter is fixed at 1 inch the same as the original SLAC design. The cell is composed of a pair of chokes. The junction from the pipe into the groove is rounded by r2mm to reduce the surface electric field. The length of the cell is fixed at 40mm, though further optimisation of surface field is estimated when considering the reflected wave phase tuning as described later.

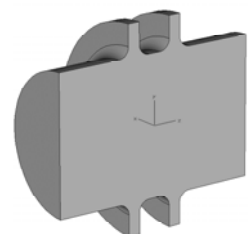


Fig. 2 Load cell shape.

Number of cells was fixed at eleven, taking the same

<sup>1</sup> E-mail: toshiyasu.higo@kek.jp

number as the original SLAC design. Fig. 3 shows the transmission properties of the cells. In order to make the load wideband, the frequency tunings of the cells are distributed.

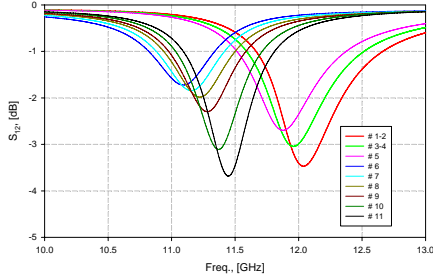


Fig. 3 Transmission performances of each cell.

### 2.3 Optimization of cell parameters

In the present design, we tried to reduce the surface electric field rather than making the heat dissipation uniform along the lossy section. To this end, an optimisation process was performed as described below. Firstly, we define a geometry factor of each cell,

$$k_i = P_i / P_N,$$

where  $i$  is the cell number,  $P_i$  – power dissipated in the  $i$ -th cell and  $N$  the number of cells in the load. Then, we can simply write a set of equations

where  $A_j$  is the transmission through cell  $i$  and  $k_{sum}$  is the

$$(1 - A_j) \prod_{i=1}^N A_i \left[ \frac{1}{\prod_{i=j}^N A_i} + \frac{\prod_{i=j}^N A_i}{A_j} \right] = \frac{k_g^j}{k_{sum}},$$

sum of all  $k_i$ . Secondly the linear functional form is assumed for  $k_i$  and calculate  $A_j$ . Then, calculate the actual field of each cell by using a 3D electromagnetic field solver HFSS and follow a multi-parametric optimization algorithm [7] to obtain a parameter set which gives the required  $A_i$  while keeping the matched condition. Then, we modify the  $k_i$  trying to make the electric field uniform. The iteration is repeated until the resultant electric field becomes uniform to proceed.

The optimized result is shown in Figs. 4 and 5.

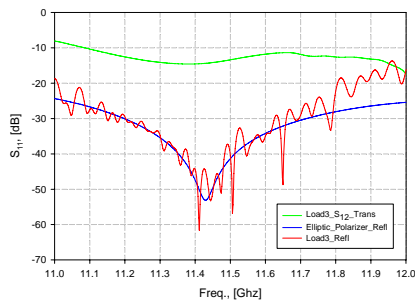


Fig. 4 The characteristics of the optimized load. The top curve is one pass insertion loss of lossy cells, the lower

smooth line the reflection from the polarizer and the last line the reflection from the whole load assembly.

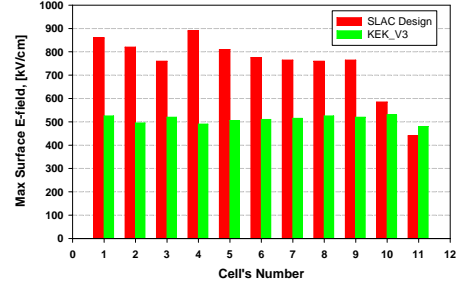


Fig. 5 Electric field along the lossy section of the present load in green bars. For comparison, the values of the SLAC load are also plotted in red bars.

### 2.4 Change of magnetic property at high temperature

Because of the possible change of the crystal characteristic structure of the magnetic stainless steel SS430 at a high temperature, the surface resistance may decrease during the high-temperature brazing processes during assembly. Fig. 6 shows the one-pass attenuation studied with a test sample equivalent to the cell #1. Four curves are those measured as of machined, after first copper brazing at 1100C, after gold brazing at 1040C and after second processing at 1100C. As shown in the figure, it was found that the first heat treatment mainly determines the decrease of resistance. The change is not very big but we designed the load based on this final characteristics.

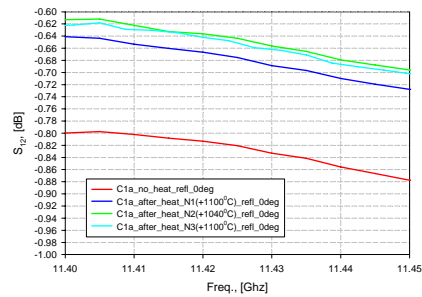


Fig. 6 Material change due to a series of high-temperature processes.

### 2.4 Polarizer

As shown in Fig. 1, a smooth geometrical transition is formed from the rectangular cross section to the circular one by connecting both periphery shapes with straight lines. The linearly polarized  $TE_{11}$  mode to the circularly polarized  $TE_{11}$  mode is performed with inserting an elliptical shape in between with 45 degrees rotated. Due to its smoothness, the matching frequency dependence is wider as shown in Fig. 7.

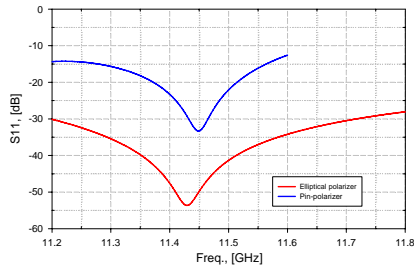


Fig. 7 Comparison of two types of TE<sub>11</sub> mode circular polarizer, pin-type (SLAC) and smooth elliptical type (present one).

### 3 FABRICATION

An RF load of the present design has been fabricated at KEK. The process of load fabrication consists of three steps as listed below. The lossy load cells are processed in a high-temperature treatment at least three times.

#### Polarizer part

1. Polariser parts are made of oxygen-free copper. The inside shaping is made by wire electric discharge machine. These parts are cleaned by chemical polishing.
2. These parts are brazed with gold-copper alloy at a temperature at 1040C.

#### Lossy stainless steel part

3. The lossy magnetic stainless-steel parts are made by turning lathe. The surfaces were cleaned by chemical polishing.
4. These parts are brazed to form a stack of lossy cells. This brazing is done with copper metal at 1100C.
5. Water cooling jackets are brazed on lossy cells.

#### Final assembly

6. All sub-assembled parts are brazed at around 1040C.
7. Vacuum pumping port flange is TiG-welded.



Fig. 8 Parts for the present load. Left: elliptical polarizer and right: lossy load cell.

The final matching performance of the load is shown in Fig. 9. A smooth line is for polarizer itself, while the other two lines are those for the whole load, one by calculation and one by experimental values. The matching at 11.4GHz is better than 40dB and and the

bandwidth below -20dB is 1GHz.

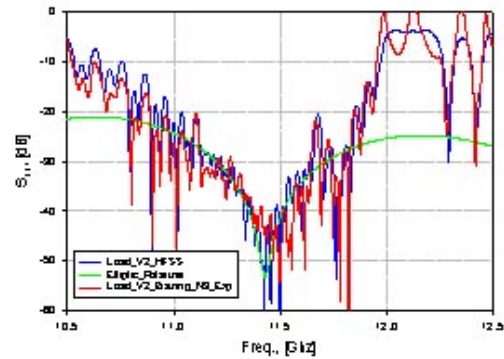


Fig. 9 Final matching performance of the present load.

### 4 DISCUSSION

The degradation of the lossy property of magnetic stainless steel was clearly observed and it is not too large so that we can use the material. A design of -40dB matching with 1GHz bandwidth below -20dB was established. The load has been fabricated and recently tested in high power. It was processed easily beyond 50MW with a pulse width of 400ns [4], proving that it is a good candidate for X-band RF high-power load.

### REFERENCES

- [1] S. G. Tantawi and A. E. Vlieks, "Compact X-band High Power Load Using Magnetic Stainless Steel", Proc. 1995 Particle Accelerator Conf., p. 2132.
- [2] W.R. Fowkes, E.N. Jongewaard, R.J. Loewen, S.G. Tantawi and A.E. Vlieks, "An All-Metal High Power Circularly Polarized X-Band RF Load", Proc. 1997 Particle Accelerator Conf., Vancouver, Canada, 1997.
- [3] D. Schultz, C. Adolphsen, D. Burke et al., "Status of a Linac RF Unit Demonstration for the NLC/GLC X-band Linear Collider", Proc. 9-th European Particle Accelerator Conference, EPAC'04, Lucerne, 5-9 July, 2004.
- [4] K. Watanabe et al., "X-band High Power Component Study for High Gradient RF Linac", 20P080, in this conference.
- [5] M. Ross, Private communication.
- [6] H. Sakai et al., "Measurement of the surface resistance of iron, stainless steel and Kanthal at 3~16GHz range", JLC-NOTE No.40, 1993, in Japanese.
- [7] R.HOOKE, T.A.JEEVS, "Direct search solution of numerical and statistical problems", Journ. Ass. Comput. Mech., 8, 1961.